Possible universal transitional scenario in a flat plate boundary layer: Measurement and visualization

C. B. Lee*
Laboratory of Fluid Mechanics, Department of Engineering Mechanics, Tsinghua University, Beijing 100084, China and State Key Laboratory for Turbulence Research (SKLTR), Peking University, Beijing 100871, China
(Received 2 July 1999; revised manuscript received 19 October 1999)

An experimental investigation was undertaken to reveal the characteristic flow structure in the regime of nonlinear boundary layer instability and onset of turbulence. A controlled Tollmien-Schlichting wave was introduced into a two-dimensional boundary layer over a flat plate to study the growth and evolution of the controlled disturbances using both hot film measurements and an improved hydrogen bubble visualization technique. The results demonstrate that the actual breakdown of the laminar boundary layer and the breakdown of the Λ vortices do not imply the immediate onset of turbulence. Rather, the onset occurs later with the breakdown of the long streaks. Therefore, an alternative transitional scenario was developed.

PACS number(s): 47.27.Cn

I. INTRODUCTION

The problem of the onset of turbulence in a flat plate boundary layer has attracted the attention of investigators for more than a century. Despite its complexity, interest in the laminar-turbulent transition has increased during the past few decades owing to its importance in both fundamental and applied aspects of classic physics. Boundary-layer flow has been a canonical flow. Theoretical and experimental studies have been discussed in various books and reviews [1–8]. The first physical study of laminar flow breakdown in the boundary layer was carried out by Schubauer and Skramstad [9]. This work served as the experimental basis for the concept of hydrodynamic instability and provided the first details of the nonlinear mechanisms of transition. The fundamental experiments conducted by Schubauer *et al.* [10] and Klebanoff *et al.* [11] laid the foundation for many ideas about the nature of laminar boundary-layer breakdown. Klebanoff *et al.* [11] studied the mechanisms of laminar flow breakdown in detail and critically evaluated the applicability of a series of theoretical models and hypotheses. Almost simultaneously, Kovasznay *et al.* [12] investigated three-dimensional flow velocity and vorticity in the same transitional region. Hama and Nutant [13] complemented hot-wire measurements with visual observations using the hydrogen bubble flow visualization technique. Based on these observations, White [14] summarized the *K* regime (*K* stands for Klebanoff) of boundary-layer transition as the following sequential stages: (i) Stable flows; (ii) unstable Tollmien-Schlichting waves; (iii) formation of three-dimensional waves and vortices; (iv) breakdown of vortices; (v) formation of turbulent spots; (vi) developed turbulence.

The famous experiments of Schubauer and Klebanoff [10] and Klebanoff *et al.* [11] showed that the nonlinear wave development at the later stages further downstream is characterized by the appearance of powerful flashes of disturbances on velocity oscilloscope traces in the form of narrow spikes. Extremely careful experiments performed by Kachanov *et al.* [15] revealed the appearance of multiple spikes, which are due to high-frequency flow structures, on the velocity oscilloscope traces (see also [8]).

Williams *et al.* [16] found that a vortex loop forms just before the spike formation in the *K* transition. Nishioka *et al.* [17] experimentally studied the local secondary instability and compared the observations with linear calculations. Asai and Nishioka [18] numerically and experimentally investigated the process of the formation of peaks and valleys. They found a threshold character for the *K* transition in a plane channel flow. Kachanov [8] suggested some new hypotheses concerning the formation of spikes and multiple spikes on the time traces. The structures of the boundary-layer flows are considered to be composed of toothlike structures in the near-wall region, spike solitons at the external edge of the boundary layer, and chaotic flows in the middle of the boundary layer. Very recently, Lee [19–21] and Lee *et al.* [22] have proposed a new scenario for transition which involves the formation of both low- and high-frequency vortices. This paper concentrates on experimental observations in the later stage of the nonlinear breakdown of the boundary layer in controlled transition, and presents direct evidence towards establishing a possible universal transitional scenario in boundary layers.

II. EXPERIMENTAL TECHNIQUES AND FACILITIES

A schematic of the experimental setup is given in Fig. 1. The experiments were conducted in a new low-turbulence level water channel in the State Key Laboratory for Turbulence Research (SKLTR) in Peking University at a free stream velocity $U_0 = 17.0$ cm/s with a turbulence level around 0.1%. The cross section of the channel is 600×400 mm^2, and the test section is about 6000 mm long. A flat plate with a chord length of 1.8 m, a span of 0.8 m, and a thickness of 15 mm was mounted vertically. Part of the flat plate is above the water surface because the top of the channel is open. The leading edge was composed of two 90° arcs with different radii. The plate was mounted in the test section at zero angle of attack. The streamwise and spanwise

*Electronic address: cblee@tsinghua.edu.cn

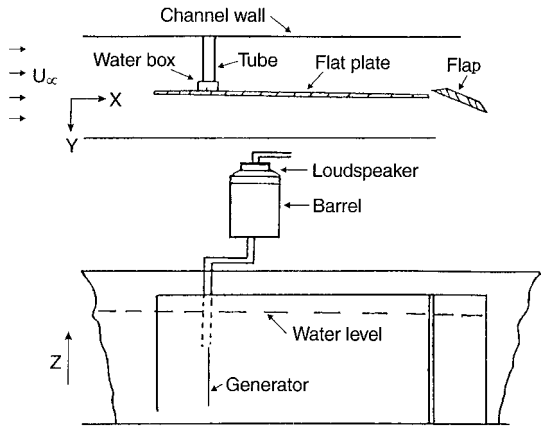

FIG. 1. Experimental setup.

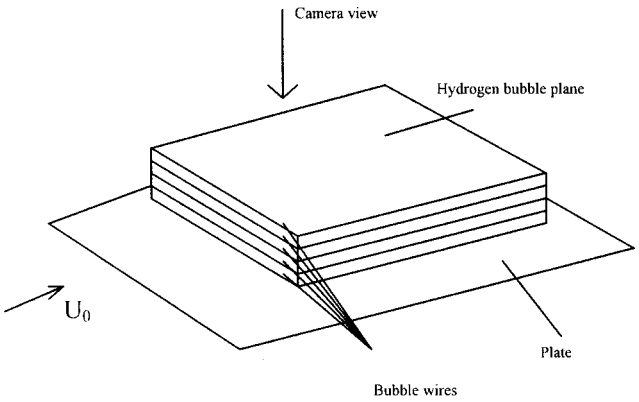

FIG. 2. Visualization techniques.

pressure gradients were nearly zero far from the leading edge. A downstream flap was used to make the flow more uniform.

The disturbance generator (Tollmien-Schlichting wave generator) was a spanwise slit in the plate of length 150 mm and width 1 mm on the working side mounted at a distance $x=200$ mm from the leading edge of the plate. Water was periodically pumped in and out of the slit at a frequency of 2 Hz. A water tank was connected to both the slit and two tubes on opposite sides of the plate. A loudspeaker was set on top of a round barrel with the two tubes mounted on the outer edge of the barrel's bottom. The instability waves had a frequency of 2 Hz and an amplitude of 1.6% of the free stream velocity U_0 as set by the voltage input to the loudspeaker. The development of the disturbances in the boundary layer and the structure of the mean flow were investigated with a hot-wire anemometer made by Kanomax Company. The hot films were made by TSI. The sensitive part of the probe was less than 2 mm long.

Experimental data were acquired from $x=248-700$ mm. At each measured point, three characteristics were measured: the mean value of the streamwise velocity U_0, and the amplitude and phase of the streamwise disturbance velocity, u, filtered at the fundamental frequency. The distributions of these characteristics were measured along the streamwise direction (x), normal to the plate (y), and along the spanwise direction (z).

Along with these measurements, an improved hydrogen bubble technique was used to carefully visualize the flow structures. Complete visualization of the flow structures was accomplished by placing the hydrogen bubble wire at positions from $x=250-700$ mm in steps of 50 mm and from $y=0.5-6$ mm in steps of 0.25 mm. This technique made it possible to clearly visualize the spatial flow structures. As shown in Fig. 2, different sections in the plan view were obtained by placing the electrode wire at different y positions. If the flow was laminar, several hydrogen bubble planes were obtained (Fig. 2). Continuous plan views of hydrogen bubbles were produced to visualize the flow structures.

The water temperature during the experiments was about 20 °C. Constant water temperature was obtained by starting the water channel more than 9 h before each test. The kinematic viscosity is 1.01×10^{-6} m^2/s and the Reynolds number per meter of length is 1.7×10^5.

III. MEAN FLOW WITHOUT EXCITATION

The velocity profiles U/U_0 in the undisturbed boundary layer are shown in Fig. 3, at $x=300$, 400, and 600 mm in the ''peak positions'' ($z=0$). The definition of the ''peak position'' was suggested in the classic study of Klebanoff [11]. All these results are in excellent agreement with the Blasius profile, which is the necessary condition for controlled transition. The maximum deviation of the experimental points from the theoretical curve is less than $\pm1\%$. The streamwise distributions of the boundary-layer displacement thickness δ_1 (Fig. 4) also agree very well with theoretical values. These results also confirm the reliability of studying transition in the new SKLTR water channel.

IV. EXPERIMENTAL RESULTS

A. Preliminary results with excitation

The perturbations distort the mean velocity profile in the vicinity of the ''peak positions'' ($z=0$) (Fig. 5). Outside of this region ($z=20.7$ mm), the mean velocity profiles in the ''initial'' section remain very close to the Blasius profile.

The normal to wall profile of the fundamental wave amplitude measured by the hot-film anemometer at $x=250$ mm, $z=0$ is shown in Fig. 6. In the initial section the

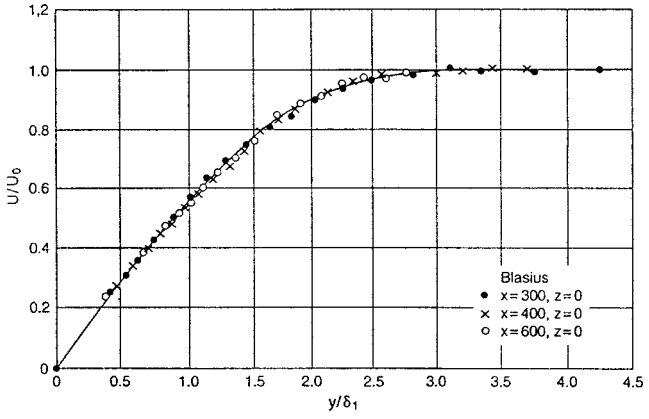

FIG. 3. Blasius profiles at different x positions without excitation.

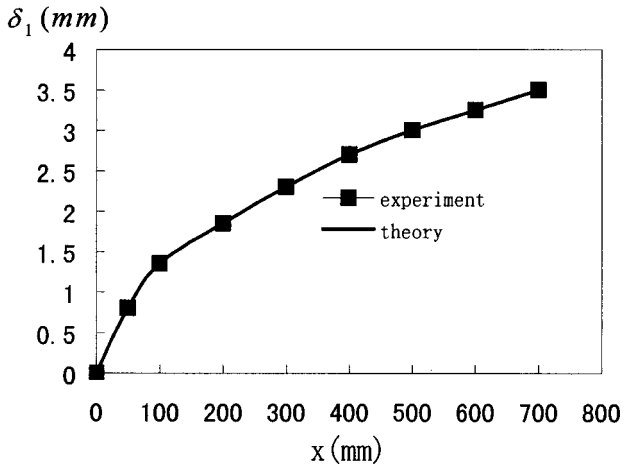

FIG. 4. Boundary-layer displacement thickness variation with streamwise coordinate without excitation.

disturbances are almost harmonic in time with weak disturbances by the second or third frequency harmonics. The profiles have a shape typical of a nearly two-dimensional linear Tollmien-Schlichting wave. However, the disturbance amplitude is already so large here that the nonlinearity is quite significant. Figure 7 shows the same profile at $x=400$ mm, $z=0$. The disturbance amplitude is even larger. The amplitude distributions along the x direction are shown in Fig. 8. Positions A, B, and C noted in the figure are the different downstream positions at which detailed observations were made, with position A corresponding to the departure from the linear theory, position B to the location of the Λ-vortex breakdown, and position C to the breakdown of the long streak. The regions from departure to breakdown of the Λ structure and from there to the long streak breakdown are of principal interest.

In the initial region with relatively low local Reynolds numbers, the instability wave (i.e., boundary-layer eigenoscillations, usually called a typical Tollmien-Schlichting wave) and its evolution can be seen from left to right in Fig. 9. As the figure clearly shows, the Tollmien-Schlichting (TS) wave develops into a Λ structure and later into several secondary high-frequency vortices. In this and all the following photos the flow is from left to right. This figure shows the typical characteristics of the K regime of boundary-layer transition as obtained in [11].

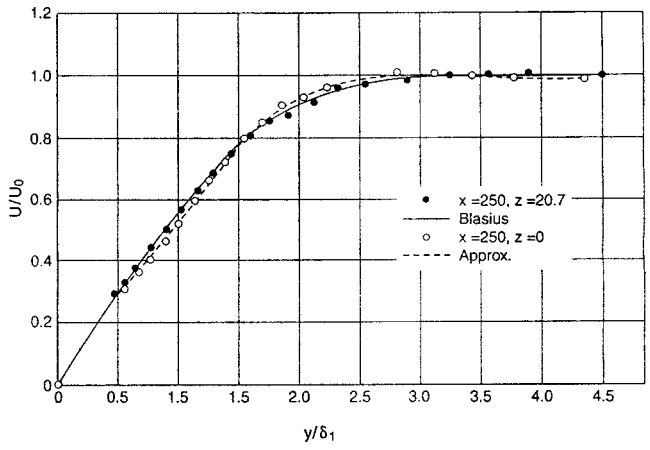

FIG. 5. Velocity profile with excitation.

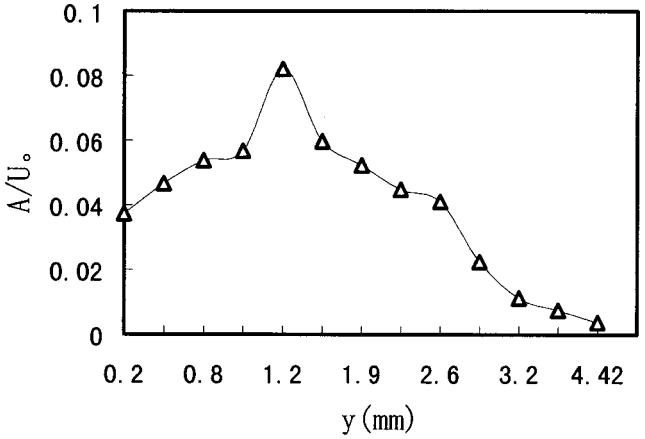

FIG. 6. y profile of the wave amplitudes at $x=250$ mm.

B. Organized flow structures

Figure 10 shows the (x,z) sectional flow structures at different y positions from the near-wall region to the outer layer. If the hydrogen bubble wire is placed very near the wall, a low-speed streak appears ($A\uparrow$) in the ''peak position'' [see Fig. 10(a)]. In addition to the low-speed streaks, a long streak ($B\uparrow$) is present at the ''peak positions'' and several arclike pairs appear on both sides of the long streak (each pair contains two arclike structures which are nearly symmetric on the two sides of the long streak). Placing the hydrogen bubble wire close to the wall at $y=1$ mm reveals a butterflylike structure [Fig. 10(b)]. The head of the Λ structure disappears and a new ''rhombuslike'' structure ($B\uparrow$) is present at the center of the ''peak position.'' When the hydrogen bubble wire is shifted slightly to $y=1.5$ mm, both a Λ structure ($C\uparrow$) and a ''rhombuslike'' structure ($B\uparrow$) within the Λ structure appear, Fig. 10(c). The Λ structure [Fig. 10(d)] is clearly seen when the wire is at $y=2.0$ mm. Almost all the structures visualized here appear at the frequency of 2 Hz. In Fig. 10(a) the long streak appears nearly at the center of the ''butterflylike'' structure (''peak positions'' [10]), and part of an arclike structure appears on both sides of the long streak at a frequency of 2 Hz. The observations show that the Λ structure cannot induce these kinds of arclike structures. A closed vortex is formed as a result of two arclike structures connecting with a low-speed streak on

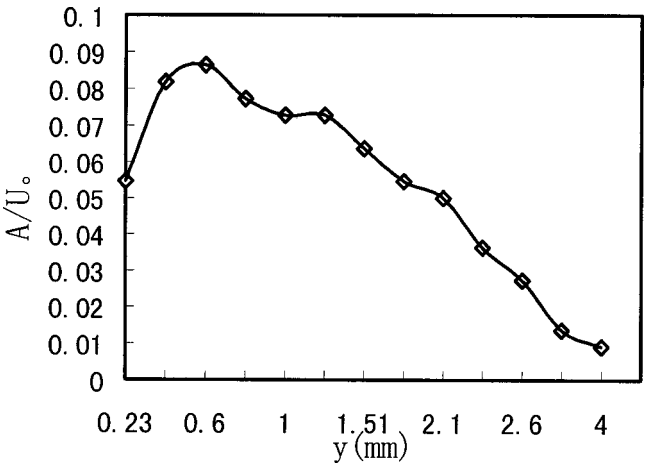

FIG. 7. y profile of the wave amplitudes at $x=400$ mm.

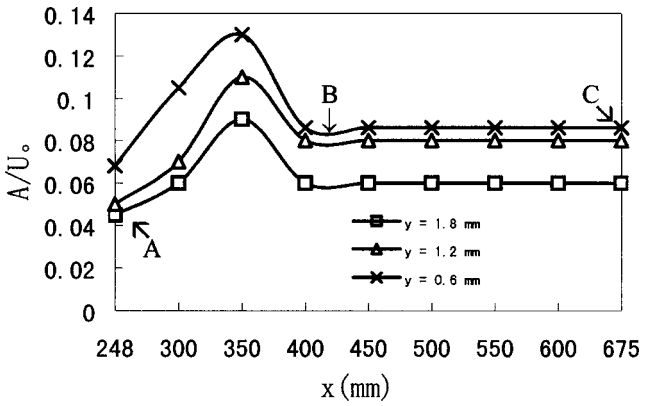

FIG. 8. Amplitude distributions in the x direction.

their left-hand side in the near-wall region and connecting with a Λ structure on their right-hand side. The Λ structure is part of the total flow structure. The ''rhombuslike'' structure lies at the center of the butterflylike structure (Fig. 10). The ''rhombuslike'' structure was referred to as solitonlike coherent structures (CS solitons) in our previous works [19,20].

The time interval must be selected carefully to obtain the different photos in Fig. 10. Time interval should be decreased to as short as possible since all the structures periodically appear and since the distance between two neighboring y positions is short (0.25 mm). At first, we chose which photos taken at two neighboring y positions are in the same period. Then we chose the best-fit two photos with the smallest time interval from the total of 24 photos (the camera frames per second and the period of the flow structures was 0.5 s, so 12 frames could be obtained per period at each y position). The minimum time interval was less than 0.04 s. In addition, the time interval was also related to other information to have the desired fundamental wave far from the ''peak position'' appear at all stages of the transition. With a proper time interval, visual observations could be used to redraw the flow structures as in Lee [19]. In Appendix A, the redrawn picture will be given.

The side view of similar structures was obtained by Hama and Nutant more than 36 years ago [13], as discussed in Lee [19,20].

C. The CS solitons and their properties

The CS solitons suggested by Lee [19,20], which are different from those observed by Kachanov [8], are typically three-dimensional wave packets, although they have the same frequency as the TS waves. The spanwise distributions

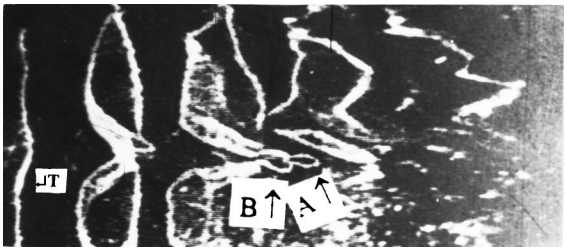

FIG. 9. TS wave ($\leftarrow T$) and its evolution to Λ structure ($C\uparrow$) and small scale vortices ($A\uparrow$ and $B\uparrow$). The figure is 1/4.3 of the actual size and the flow is from left to right for x equal to 250 mm.

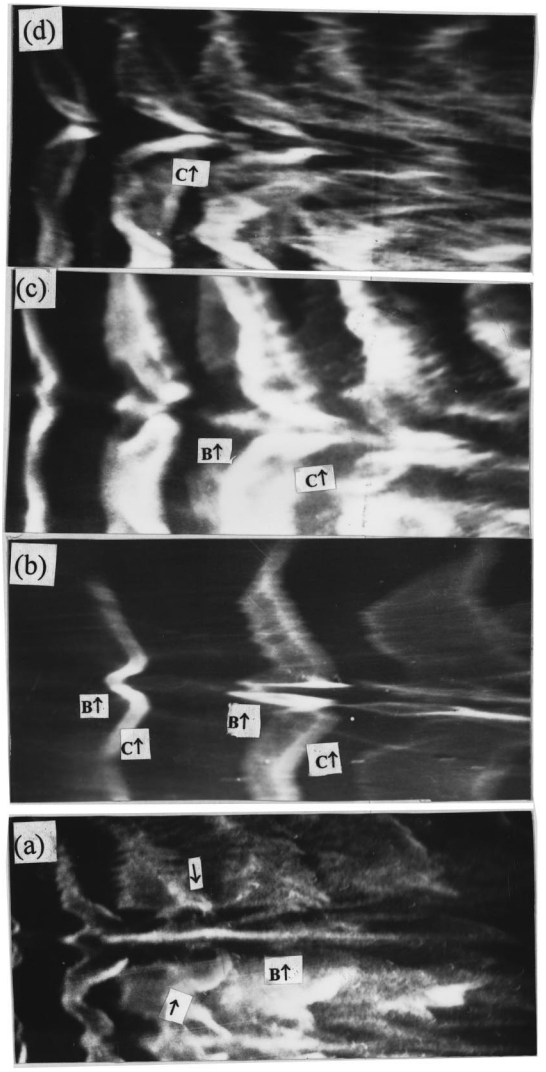

FIG. 10. Flow structures in different x-z plan views (1/3.8 scale of the actual photos at x equal to 350 mm). (a) Low-speed streak ($A\uparrow$), long streak ($B\uparrow$), and arclike structures ($\uparrow\downarrow$) at $y=0.5$ mm. (b) Butterflylike structure ($B\uparrow$) and Λ structure ($C\uparrow$) at $y=1.0$ mm. (c) Butterflylike structure ($B\uparrow$) and Λ structure ($C\uparrow$) at $y=1.5$ mm. (d) Λ structure ($C\uparrow$) at $y=2$ mm.

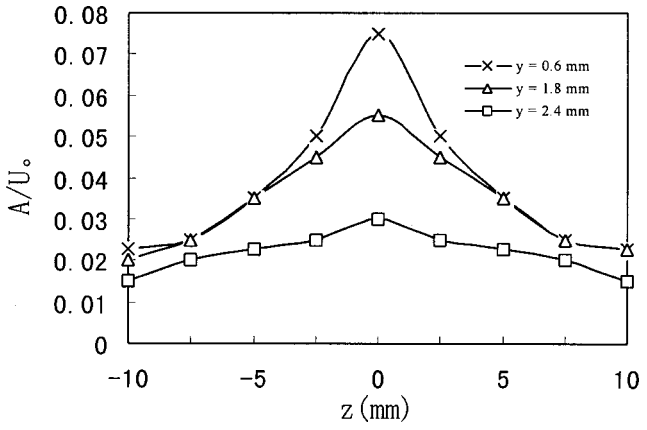

FIG. 11. Amplitudes of disturbances of CS solitons at different y positions ($x=400$ mm).

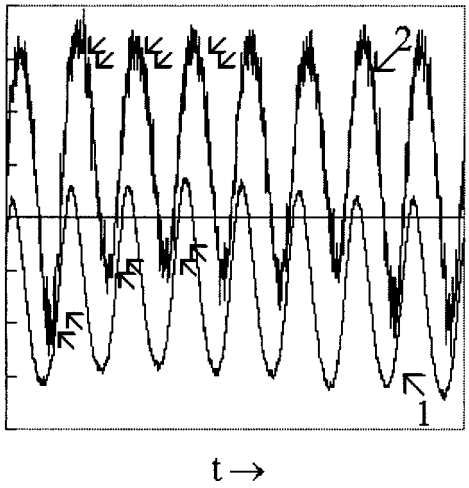

FIG. 12. Oscilloscope traces of velocity disturbances at different x for $y=1.6$ mm. Curves 1 and 2 are for $x=248$ and 350 mm, respectively. The time scale of one period is 0.5 s.

of the amplitudes of the CS solitons can be seen in Fig. 11 at different y positions. The graph shows a strong spanwise localization of the CS soliton, which developed from TS waves as a result of resonance between two oblique waves.

Figure 12 shows the time traces measured at $x=248$ and 350 mm for the same $y=1.6$ mm. At $x=248$ mm, additional spikes are not found because both the Λ structure and the low-speed streak have not yet appeared. The fluctuations in curve 1 are generated by just the CS solitons. At $x=350$ mm, additional spikes are found in both the ''peak'' and the ''valley'' on the time trace as indicated by the arrows. Additional spikes in the ''peak'' on the time traces were generated by Λ vortices and the spikes in the ''valley'' by the low-speed streaks. The main fluctuations in this curve were still generated by the CS solitons called ''rhombus-like'' structures in Fig. 10. The measured results (curve 2 in Fig. 12) and the observations in Fig. 10 agree very well with each other qualitatively. Figure 13 shows a typical set of oscilloscope traces measured at various distances from the wall. Two main features can be seen. (i) The main fluctuations are present not only in the near-wall region but also in the outer layer. (ii) The phases of these fluctuations are nearly the same at all y locations. Because the fluctuation amplitudes in the near-wall region ($y\leqslant 3.24$ mm) are much greater than those in the outer layer, the scales of the fluctuations for the first eight positions were reduced so that all the time traces would fit in the same figure. Referring to Figs. 10, 12, and 13, the spatial scales of the CS solitons in the x direction are greater than that of the leading edge of the Λ structures at the ''peak position.'' Since the low-frequency fluctuations have the same frequencies at different y positions, the low-frequency, high-amplitude fluctuations in Fig. 13 were generated by the CS solitons at different y positions. In fact, the additional spikes in Fig. 13 occurred in curve 2 of Fig. 12. The reason the spikes are not clearly observed is that the scale used in the figure is not good for seeing these additional spikes. Figure 14 shows the evolution of the CS solitons from their formation to their later stage before breakdown. The main shapes of the CS solitons remain practically unchanged further downstream.

In summary, experimental results show the following.

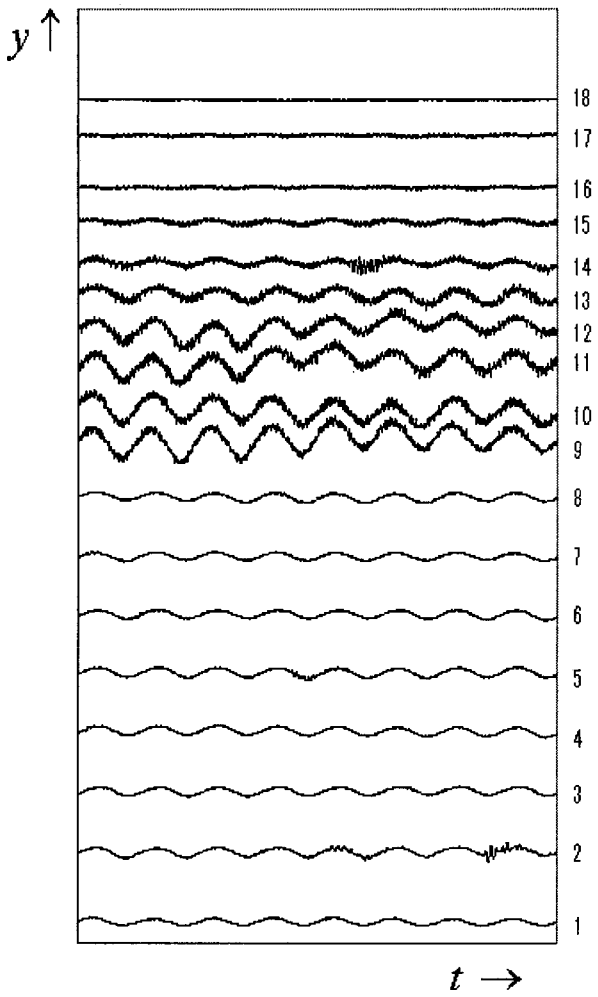

FIG. 13. Oscilloscope traces of velocity disturbances at various distances from the wall at $x=400$ mm. Curves 1,2, . . . ,18 for $y=0.22$, 0.49, 0.75, 1.0, 1.25, 1.88, 2.27, 3.24, 3.62, 4.0, 4.5, 4.99, 5.5, 6, 7, 7.5, 8.12, and 10.25 mm (the curves from 1 to 8 are divided by 8 so they can fit in the figure).

(i) The CS solitons are present not only in the near-wall region but also near the external part of the boundary layer.

(ii) The main features of the CS solitons remain unchanged before their breakdown, which is why they are called CS solitons.

D. Chain of ringlike vortices

The experimental observations show that a chain of ringlike vortices composed of four vortices appears at the same frequency as the TS wave, at the tip of each Λ structure (part of the closed vortex). The formation process for these ringlike vortices is shown in Fig. 15. The first ringlike vortex appears at $x=430$ mm from the leading edge. The pictures were obtained with the cathode wire positioned parallel to the wall. The appearance of the first, second, and third vortices is clearly seen in Figs. 15(a)–15(c). The fourth one was seen in the video. This process is a typical breakdown of a Λ structure, which represents a periodic change instead of a random change.

Figure 16 shows high-frequency fluctuations associated with the breakdown of a Λ structure and the formation of the chain of ringlike vortices. The multiple spikes are generated

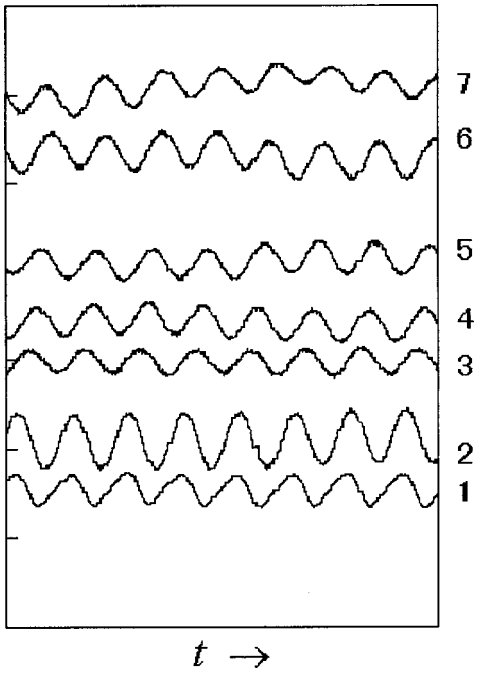

FIG. 14. Oscilloscope traces of velocity disturbances at different x for $y=0.6$ mm. Curves 1,2, . . . ,7 for $x=300$, 350, 400, 450, 500, 550, and 600 mm.

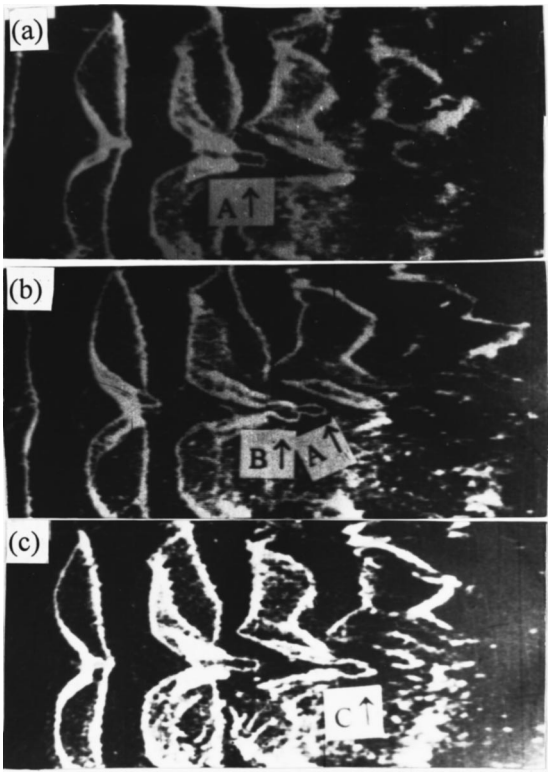

FIG. 15. Formation of a chain of ringlike vortices ($\frac{1}{4}$ scale from the actual size for x from 420 mm, $y=1.0$ mm). (a) First ringlike vortex formation ($A\uparrow$) ($t=$ ''0'' s). (b) Second ringlike vortex formation ($B\uparrow$) ($t=0.166$ s). (c) Third ringlike vortex formation ($C\uparrow$) ($t=0.291$ s).

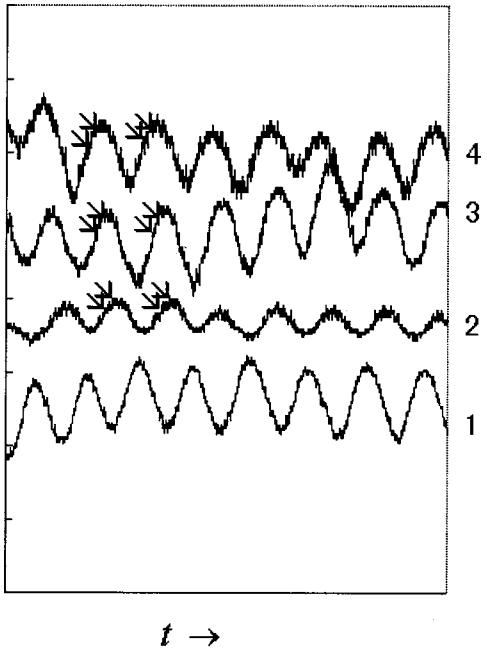

FIG. 16. Oscilloscope traces of velocity disturbances at various distances from the wall at $x=450$ mm. Arrows indicate the multiple spikes generated by a chain of ringlike vortices. Curves 1 to 4 for $y=0.61$, 1.0, 1.8, and 3.4 mm.

by only the first two vortices in the chain because the third and fourth vortices do not appear before $x=450$ mm.

In Fig. 17, positive and negative spikes are periodically induced by the chain of ringlike vortices and the closed vortex. Each ringlike vortex induces one positive spike and one negative spike, i.e., a spike pair. Five spike pairs appeared, which is one more than the number of ringlike vortices, implying that the closed vortex generates an extra spike pair. The spike on the left-hand side of the pair on the measured time traces is generated by the right-hand side of the part of

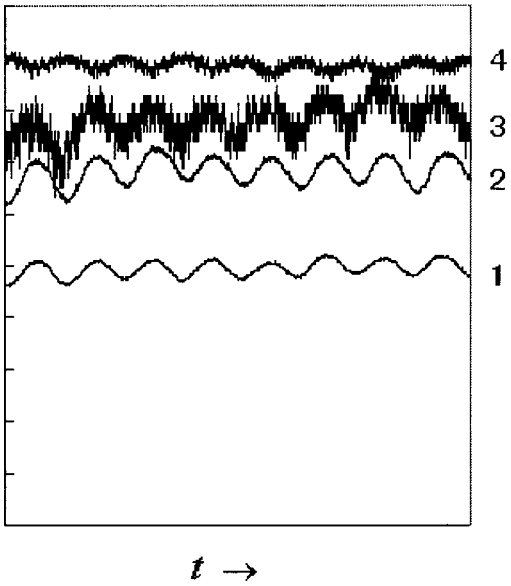

FIG. 17. Oscilloscope traces of velocity disturbances at various distances from the wall at $x=500$ mm. Curves 1 to 4 for $y=0.22$, 2.1, 3.2, and 8.0 mm.

the vortex in the visualization figure and vice versa. Because the plane spanned by a ringlike vortex is inclined at more than 45° to the wall, the time traces of the velocity at a fixed *y* position do not show all the pairs. The inclination angle of the vortex plane can be seen clearly from the video and movie taken simultaneously during a test. In the near-wall region, the spike corresponds to the right side of the time traces in one period because the local velocity is only affected by the left part of the ringlike vortices. The spike pairs appear on the time traces in the central layer (Fig. 16 and Kachanov [8]).

Generally, the main features relevant to the chain of ringlike vortices are as follows.

(i) The chain of ringlike vortices appears with the same frequency as the fundamental wave.

(ii) The traces show single, double, or more spikes which influence the flow in the near-wall region and the flow near the external part of the boundary layer. These kinds of multiple spikes are generated by the chain of ringlike vortices and the closed vortex.

The time interval between the neighboring ringlike vortices in the chain is equal to that of the neighboring spikes on the measured time traces. The ringlike vortices separate from the tip of the Λ structure and the two legs of the vortex are reconnected into a closed ringlike vortex by the law of vortex dynamics (Fig. 15). This physical process, which is similar to the self-induction effects observed by Moin *et al.* [23], was suggested by Kachanov [22]. The present experiments show that a ringlike vortex in the chain is not directly separated from the tip of the Λ structure during the vortex formation. Figure 18 shows the formation process of a ringlike vortex, which demonstrates that this structure is directly separated from the border of a CS soliton inside the butterflylike structure. Figure 18(a) shows the leading edge of the vortex ($1\rightarrow$) inside the Λ structure ($C\uparrow$). Figure 18(b) shows that the head part of the vortex is separated from the border of the CS soliton ($B\uparrow$) and this structure appears in the mouth of the Λ structure. Unfortunately, the photos are not as clear as the moving process seen in the video. A typical vortex shape is formed ($\uparrow 1$), Fig. 18(c), and the vortex is accelerated by the Λ structure and its rotational speed increases. In Figs. 18(d) and 18(e) the vortex ($1\uparrow$) moves downstream at a higher convection velocity than that of both the Λ structure and the CS soliton. The angle between the plate and the plane spanned by the vortex increases ($>70°$) as clearly shown in the movie and video. This process appears at a frequency of 2 Hz. The physical mechanism for the formation of the rest of the vortices is not yet clear. They probably result from a physical mechanism similar to the ringlike vortex. However, further experimental evidence is necessary. The Ω-shaped part of the vortex suggested by Knapp and Roache [24] is the first ringlike vortex observed here.

Falco [25] identified a relatively small-scale coherent motion, which he labeled a ''typical eddy.'' He proposed that the eddy was the direct result of a superburst in the outer region of a smoke-filled, turbulent boundary layer. Lee [20] found a chain of ringlike vortices in the outer region of the turbulent boundary layer, which are very similar to that in Fig. 15.

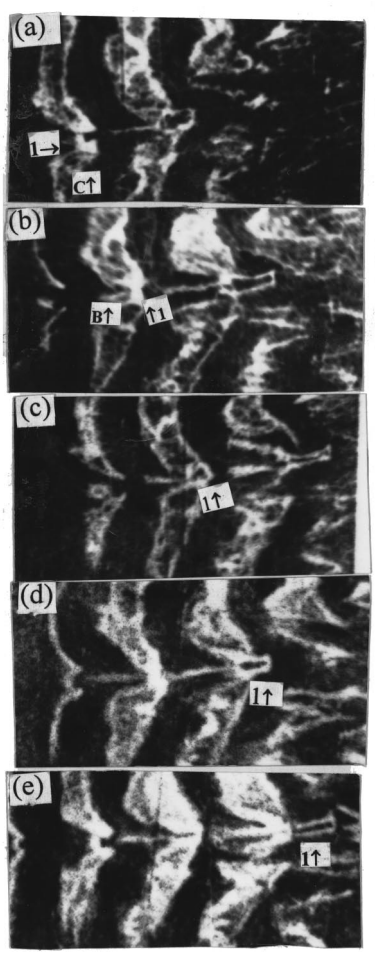

FIG. 18. Formation of one of the ringlike vortices in a chain of ringlike vortices (1/5.0 scale from the actual size). (a) Leading edge of the vortex ($\rightarrow 1$) inside the Λ structure ($C\uparrow$) ($t=$''0'' s). (b) The vortex separated from ($\uparrow 1$) separated from a CS soliton ($B\uparrow$) ($t=\frac{1}{2}$ s). (c) Vortex is formed ($t=\frac{1}{6}$ s). (d) Vortex is clearly shown ($t=\frac{1}{4}$ s). (e) Vortex stretched ($t=\frac{1}{3}$ s).

The effect of the formation of the vortex ring along the border of the CS soliton in natural transition [19] should also be analyzed. The high-shear layers and the closed vortex formation along the borders of the CS solitons occur due to mass conservation and the low convection speed of the CS solitons. On the right-hand side of the CS soliton, the flow sweeps down from the free stream to the right side of the CS soliton. The flow upstream of the CS soliton would sweep down to the near-wall region on the left-hand side of the CS soliton. Consequently, the high-shear layer and the closed vortex form along the border of the CS soliton. As mentioned by Lee [19], the vortex-ring formation process along the border of the CS soliton can be seen in the work by Hama *et al.* [13]. An improved experimental study for understanding the physical process which provided further information on the formation of the chain of ringlike vortices will be discussed in a later publication.

The mechanism for a vortex to separate from a CS soliton is not yet clear. The separation may occur because the vortex convection velocity is greater than the velocity of the CS soliton because of a lift-up effect such as the bursting processes in a turbulent boundary-layer flow [26]. Additional

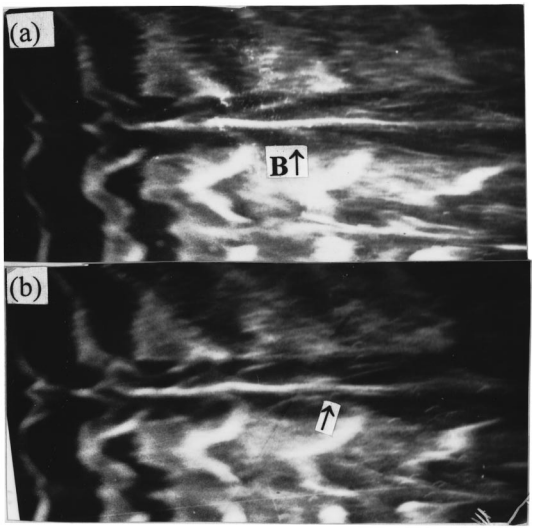

FIG. 19. A long streak ($B\uparrow$) and its breakdown ($\uparrow$) (1/3.8 scale from the actual size). (a) Long streak. (b) Breakdown.

evidence is needed to confirm this preliminary explanation. An additional experiment for understanding the rapid increase of the angle between the flat plate and the vortex plane is currently underway.

More detailed information is necessary to better understand the present results. Because different parts of a flow structure and different flow structures appear in different ways depending on where the hydrogen-bubble wire is mounted, more attention should be paid to check the flow structures and determine their properties. Several plan-view sections or side-view sections must be used to produce clear three-dimensional flow structures.

E. Long streaks in a transitional boundary layer

A long streak is present in Fig. 19 which was obtained with a cathode-wire position of $x=350$ mm and $y=0.5$ mm. The structure is modulated in time with the fundamental frequency. This kind of long streak has never been observed experimentally in the two known ''normal'' regimes of the boundary-layer transition, namely the *K* regime or the *N* regime [8]. The breakdown of the long streak happens regularly, as shown in Fig. 19(b).

The long streak (Fig. 19) in a transitional boundary layer is different from that in a developed turbulent boundary layer [26,27] in several aspects. First, the long streaks in a transitional boundary layer appear in the near-wall region in the ''peak positions.'' But the long streaks in the developed turbulent boundary layer appear both in the region where the interface between the high-speed streaks and low-speed streaks often appear [27] and in the near-wall region [26]. Second, the long streaks in a transitional boundary layer represent the features of the CS solitons [19]. Direct evidence showing the formation of the long streak in the near-wall region is given in Fig. 20. Arrows $A1$ and $A2$ demonstrate the evolution of the form of the CS soliton into part of a long streak, which still has the features of the CS soliton. A complete long streak, Fig. 19, is composed of several partial long streaks as clearly shown in Fig. 21. The long streak is related to the features of the CS solitons because in the near-wall region the low-frequency, high-amplitude fluctuations of the

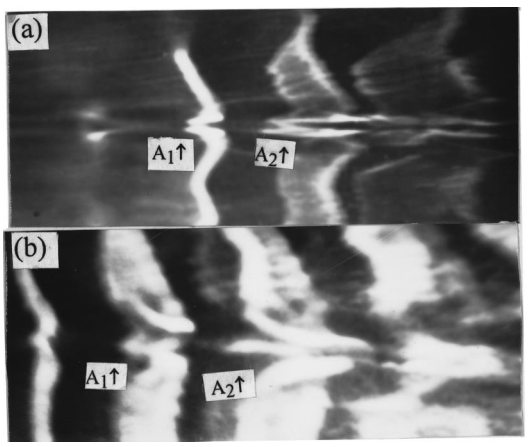

FIG. 20. From a CS soliton ($A_1\uparrow$) to a part of a long streak ($A_2\uparrow$) (1/3.8 scale from the actual size). (a) $y=1.0$ mm. (b) $y=1.5$ mm.

x component of the velocity increase the streak length (Fig. 14). Therefore, the streak not only has a convection velocity but also a high-amplitude oscillatory velocity [19,20]. The streak will spread both upstream and downstream forming a long streak. The formation of this streamwise long streak is typical of turbulent slugs, as described by Linden [28,29].

V. DISCUSSION

A. Differences between a CS soliton, a chain of ringlike vortices, and a turbulent spot

The CS solitons observed by Lee [19] differ from those by Borodulin and Kachanov [8] and the turbulent spot.

Both the visual results and the experimental measurements demonstrate the existence of the CS solitons from the initial stage of three-dimensional structure formation ($x=260$ mm) to the later stage of transition and the onset of turbulence. According to the definition of Kachanov and his co-workers [8], the CS solitons they observed are the outer part of the chain of ringlike vortices.

It is well known that a turbulent spot appears at the later stage of transition [14]. Very recently, Kachanov [8] suggested a transitional path ''without turbulent spot transition.'' Some other researchers suggested another path called ''direct to turbulent spot transition'' or ''by-pass transition'' [30,31]. The controversy has two aspects. (i) The formation process for the CS solitons and the vortices has not been clearly visualized in [19]. (ii) The main differences between the turbulent spot and the CS soliton have not been clearly distinguished.

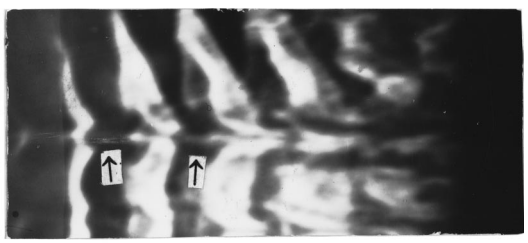

FIG. 21. A complete long streak is composed of several CS solitons ($\uparrow$) (1/4.0 scale from the actual size).

A regular turbulent spot represents the features of localized turbulence involving several mushroomlike structures [32]. The turbulent spot is very similar to several CS solitons and their bounded vortices at the same z position, but quite different from that in ''by-pass'' or ''direct to turbulent spot transition.'' Actually, the turbulent spot suggested in ''by-pass'' or ''direct to turbulent spot transition'' is the CS soliton observed in this work.

There was only one ''peak position'' in the experiment conducted by Kachanov *et al.* [8] but there were four ''peak positions'' in the experiment by Klebanoff *et al.* [11]. A real turbulent spot such as in [32] cannot form, but the CS solitons exist (see Fig. 30 in [8]). The lack of detailed visualized results in the initial stage of this structure in previous publications has prevented proper interpretation of the CS solitons in the early stage of transition. Because of the importance of this structure in a transitional boundary layer and since it was found in other flow fields, this structure can be assumed to be one of the coherent structures in transitional and nearly developed turbulent boundary layers. Furthermore, Lee [19] proposed that this structure is of a deterministic nature. CS solitons appear at conditions called controlled transition [8,20], ''direct to turbulent spot transition'' or by-pass transition [30,31], and natural transition [19]. Our recent studies [20,21] gave a new physical process for the vortex formation along the borders of the CS solitons. In fact, some differences exist between the regular turbulent spot and the structure with the same name in some ''by-pass transition'' or ''direct to turbulent spot transition'' observations.

B. Physical mechanism for the CS-soliton formation

Receptivity is defined as the mechanism by which disturbances enter the boundary layer and create the initial conditions for unstable waves. The following discussion considers which kinds of unstable waves can generate the rhombuslike CS solitons in the plan view.

The wave resonant concept has been suggested [8] on the basis of a detailed analysis of experiments by Kachanov and Levchenko [33] as well as analysis of the theoretical results by Crack [34], Zelman and Maslennikova [35], Nayfeh and Bozetli [36], Herbert [4], and others. The results obtained by Borodulin and Kachanov [8] showed that the system of the parametric subharmonic resonance, postulated within the framework of the wave resonance concept, is actually observed in the K regime of boundary-layer breakdown at the stage of spike formation. Simulations of oblique wave interactions in a Blasius boundary layer were performed by Joslin *et al.* [37]. The simulations showed that oblique wave interaction generates a strong spanwise-dependent mean-flow distortion. No two-dimensional TS waves take part in this process, but CS solitons can generate this kind of strong spanwise-dependent mean-flow distortion. The results of Williamson [38] and Williamson and Prasad [39] reveal a honeycomb pattern that is considered to be a direct result of the interaction between oblique shedding vortices and two-dimensional large-scale waves that grow in the far wake. One possible physical reason is that the CS solitons are generated by the interaction between two oblique waves. However, in this work, the CS solitons would have to be generated by the two-dimensional TS waves. A theoretical approach called ''phase-locked in'' by Wu and Stewart [40] showed that two-dimensional TS waves have a catalytic effect on the three-dimensional structure formation. The results in Fig. 20 show that the above two effects are quite possible.

Some scientists believed that the CS solitons are secondary structures generated by the Λ structures. No direct evidence in Figs. 10 and 20 showed that the Λ structures were formed before the formation of the CS soliton. The motion pictures from the video and films show that the CS solitons were formed slightly before the Λ structures. This evolution is very similar to the process suggested in [19] and [20].

Generally, the CS solitons are proposed to be the direct results of the interaction between two oblique waves and the two-dimensional TS waves are proposed to have a catalytic effect on their formation.

TABLE I. Number of vortices in one chain associated with a large-scale motion.

Sources	Name	Turbulent BL	Transitional BL
Falco [25]	typical eddy	4	
Lee [19]	no name	4	
Klebanoff [11]	no name		4
Hama [13]	no name		4
Borodulin [8]	spike solitons		4
present	CRV		4

C. Similarity between transitional and developed turbulent boundary layer

The structural similarity between transitional and developed turbulent boundary layers was first briefly discussed by Blackwelder [41]. Kachanov [8] discussed the connection between the K breakdown and developed turbulence. The flow structures in developed turbulence obtained in the works of Fukunishi *et al.* [42] and Thomas *et al.* [43] are very similar to that by Borodulin and Kachanov [8].

Three kinds of coherent structures exist in a transitional boundary layer: the CS solitons, the closed vortices, and the chains of ringlike vortices. All three structures can also be found in developed turbulent boundary layers [19,20]. Several CS solitons appear in the boundary layer in the form of a long streak in the near-wall region or in the form of a black spot in the outer layer. A closed vortex is not easily seen because of the angle between the vortex plane and the flat plate. Therefore, only part of a closed vortex is normally seen using flow visualization. The chain of ringlike vortices, which generate high-frequency fluctuations, is often considered to be chaotic flow structures because no one believes they have periodic features in a developed turbulent boundary layer, including even Falco [25]. The localized periodic features of these structures were found in a few studies [19,20] but not mentioned clearly at that time, because the present transitional boundary-layer results had not yet been obtained. Table I compares the number of the ringlike vortices in a chain in transitional and developed turbulent boundary layers. The number of the vortices in a chain associated with a large-scale motion is the same for different experiments, indicating this may be a constant. Note that Hama *et al.* [13] suggested a fourfold cascading breakdown instead

of the formation of a chain of ringlike vortices (CRV) suggested in the present paper.

Lee [20] discussed the similarity between the physical mechanisms for the structure formation in both transitional and developed turbulent boundary layers. The onset of turbulence in turbulent boundary layers was first considered as bursts by Kline *et al.* [26], Kim *et al.* [44], and Blackwelder *et al.* [45]. Their observations showed local and temporary ejections of low momentum fluid towards the wall, alternating with local generation of highly unstable instantaneous velocity distributions, resulting in turbulence bursts, which show up in the velocity oscilloscope traces as intensive high-frequency fluctuations. This burst process was also observed in transitional boundary layers [19,20].

VI. CONCLUSIONS

The present experimental study in a transitional boundary layer reveals a complete flow structure called the butterflylike structure, which consists of a CS soliton, a closed vortex, and a chain of ringlike vortices with small time scales as the basic ''building blocks.'' These results provide an improved understanding of the transitional scenario.

The experimental observations show that the multiple spikes, which were observed over one period of the fundamental wave in a transitional flat plate boundary layer, were generated by a chain of ringlike vortices and a closed vortex. The Λ structure is part of the whole butterflylike structure from the stage of the obvious three-dimensional structure formation to nearly developed turbulent flow. Inside the butterflylike structure, the CS solitons, which were observed by Lee [19,20] and referred to as ''kinks'' by Hama many years ago [13], are observed here to exist over most of the boundary layer. The observation of the chain of ringlike vortices during one period of the fundamental wave can be used to explain the physical process for the formation of the multiple spikes on the time traces measured by Borodulin and Kachanov.

Streamwise streak breakdown was considered to be a necessary but not sufficient condition for transition to occur in the oblique wave scenario [46], which was described by

$$\text{Oblique waves} \Rightarrow \text{streamwise vortices} \Rightarrow \text{streamwise streaks} \Rightarrow \text{streak breakdown} \Rightarrow \text{transition.}$$

The present experimental results suggest a different transitional path:

Oblique waves interaction with TS wave

$$\Rightarrow \text{CS soliton} \Rightarrow \begin{cases} \text{closed vortex} \Rightarrow \text{chain of ringlike vortices} \\ \text{long streak} \end{cases} \Rightarrow \text{long streak breakdown} \Rightarrow \text{transition.}$$

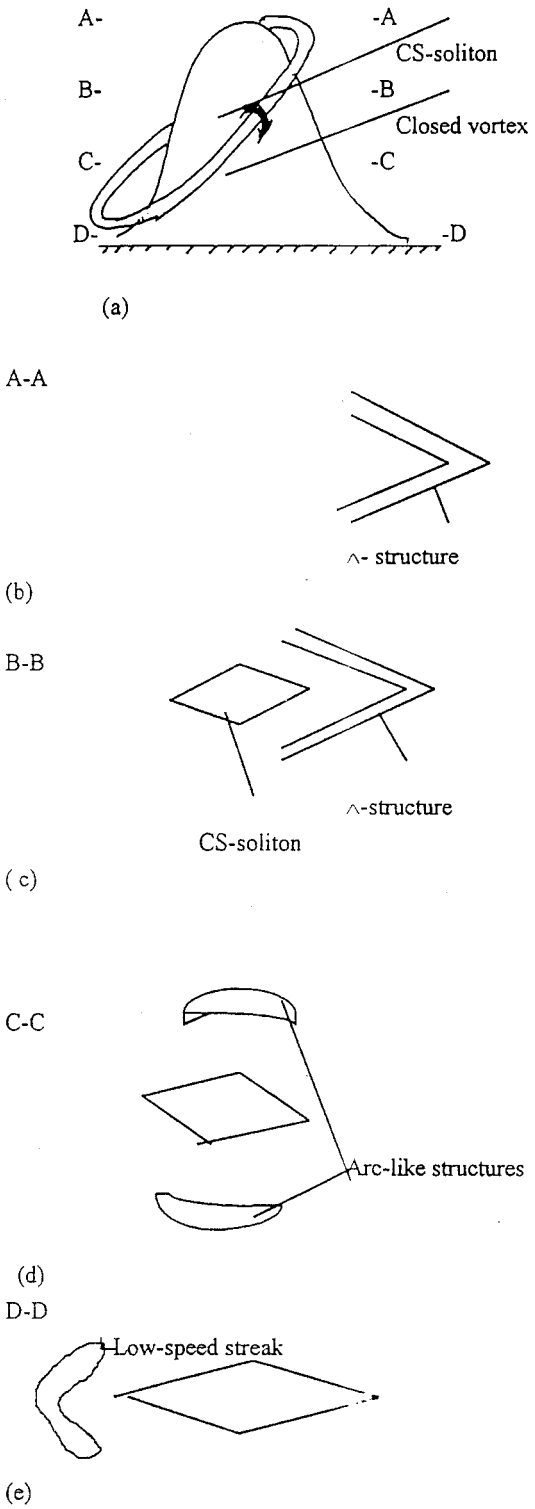

FIG. 22. Redrawn flow structures and their sectional views at different y positions. (a) Sketch of the flow structure in Fig. 10. (b) A-A sectional view, which is similar to Fig. 10(d). (c) B-B sectional view, which is similar to Fig. 10(c). (d) C-C sectional view, which is similar to Fig. 10(b). (e) D-D sectional view, which is similar to Fig. 10(a).

The universal path to transition in a boundary layer is probably related to those paths. In general, disturbances are random noise instead of regular waves, and the nonlinear nature of secondary and higher-order instabilities leads to an enormous variety of possible behaviors [30]. The mechanisms for

transition initiated by random noise cannot be easily identified, but the observation of the regularly shaped CS solitons in the *K* transition, the natural transition, the by-pass transition, and turbulent boundary layers shed some new light on this issue. A universal mechanism may exist since different environmental disturbances generate the same structures. Some studies [38–40] have suggested oblique wave interaction as a simple universal mechanism. The present experimental results and previous experiments [8,19–21] have shown that secondary and higher-order instabilities lead to a universal result which is the formation of the chain of ringlike vortices. Morkovin [30] thought that no universal evolutionary path to turbulent flow exists even in geometrically similar mean laminar shear flows. But this assertion had been made before the CS solitons were clearly seen in controlled transitions and were confused with turbulent spots in by-pass transition. Moreover, the previous hot-wire measurements such as in Kachanov [8] were not sufficiently detailed, so the flow structures were not clearly visualized and it was impossible to determine if the observed structures were induced by secondary or higher-order instabilities. The scenario called ''without turbulent spot transition'' by Kachanov [8] seems to be insufficient because several key stages of transition, such as the formation of the CS solitons, were missed.

No exceptional examples of boundary-layer flows for both different geometric conditions and different initial flow conditions [26,27,30,47,48], which have some fundamental conflicts with the present scenario for the onset of turbulence, have been found. Perhaps the bursting process observed by Kline *et al.* [26] for the onset of turbulence is the real universal transition mechanism for boundary-layer flows for different conditions. Actually, the present scenario is an improved version or an interpretation of the bursting process.

This scenario can be applied to other flows. The flow structure referred to as a spotlike vortex by Williamson [38] in a cylinder wake is similar to the CS solitons suggested here, which indicates that a wake flow is in some ways similar to a boundary-layer flow. For a Poiseulle flow, the main processes of transition are the same as those in the *K* regime of the boundary layers. Even in a separated flow [49], a wavelike structure and its bounded vortex were found. All these experimental facts show that a similar physical process exists for the formation of the wavelike structure, here called the CS soliton.

ACKNOWLEDGMENTS

We would like to thank C. Y. Feng, Y. T. Shi, Professor Q. D. Wei (SKLTR), and X. T. Du for their help during our experiments. We also thank Professor Z. M. Jin (Chinese NSF) for his very kind encouragement. Lee is grateful to Professor J. T. Stuart (FRS, UK), Professor M. Gaster (FRS, UK), and Dr. X. Wu (Imperial College) for helpful comments. The suggestions by Professor J. Z. Wu (The University of Tennessee Space Institute and SKLTR) were very valuable for improving the paper. Professor Wu has helped the author to carefully revise the manuscript. This project was supported by the Chinese NSF, RFBR under Grant No. 96-001-00001c (Russian Foundation for Basic Research), the K. C. Wang Foundation, and the Chief Foundation of the Department of Mathematics and Physics of the Chinese NSF for special support. Part of this work was supported by the Isaac Newton Institute for Mathematical Sciences, University of Cambridge.

APPENDIX A

To further understand the flow structure in Fig. 10, a redrawn picture of the sketch of the real three-dimensional flow structure is shown in Fig. 22, which was given previously in [19]. This figure also gives several sectional plane views, which are very similar to the real plan-view flow structures in Fig. 10.

The side view of the CS solitons and their bounded vortices were clearly described in [19].

[1] A. D. D. Craik, *Wave Interactions and Fluid Flows* (Cambridge University Press, Cambridge, 1985).
[2] V. N. Zhigulyov and A. M. Tumin, *Origin of Turbulence. Dynamic Theory of Generation and Development of the Instabilities of Boundary Layers* (Nauka, Novosibrisk, Siberian Division, 1987) (in Russian).
[3] A. H. Nayfeh, AIAA paper no. 87-0044 (1987).
[4] T. Herbert, Annu. Rev. Fluid Mech. **20**, 487 (1988).
[5] H. L. Reed and W. S. Saric, Annu. Rev. Fluid Mech. **21**, 235 (1989).
[6] H. Fasel, in *Proceedings of the International Union of Theoretical and Applied Mechanics on Laminar-Turbulent Transition* (Springer, Toulouse, 1990).
[7] L. Kleiser and T. A. Zang, Annu. Rev. Fluid Mech. **23**, 495 (1991).
[8] Y. S. Kachanov, Annu. Rev. Fluid Mech. **26**, 411 (1994).
[9] G. B. Schubauer and H. K. Skramstad, J. Res. Natl. Bur. Stand. **38**, 251 (1947).
[10] G. B. Schubauer and P. S. Klebanoff, NACA Report No. 1289 (1956).
[11] P. S. Klebanoff, K. D. Tidstrom, and L. M. Sargent, J. Fluid Mech. **12**, 1 (1962).
[12] L. S. Kovasznay, H. Komoda, and B. R. Vasudeva, in *Proceedings of the 1962 Heat Transfer and Fluid Mechanics Institute* (Stanford University Press, Palo Alto, CA, 1962).
[13] F. R. Hama and J. Nutant, in *Proceedings of the Heat Transfer and Fluid Mechanics Institute* (Stanford University Press, Palo Alto, 1974), pp. 77-93.
[14] F. M. White, *Viscous Fluid Flow* (McGraw-Hill, New York, 1974).
[15] Y. S. Kachanov, O. I. Taraykin, and A. V. Fyodorov, in *Proceedings of the The International Union of Theoretical and Applied Mechanics on Laminar-Turbulent Transition* (Ref. [6]).
[16] D. R. Williams, H. Fasel, and F. R. Hama, J. Fluid Mech. **149**, 179 (1984).
[17] M. Nishioka, M. Asai, and S. Iida, in *Proceedings of the International Union of Theoretical and Applied Mechanics on Laminar-Turbulent Transition* (Ref. [6]).

[18] M. Asai and M. Nishioka, J. Fluid Mech. **208**, 1 (1989).
[19] C. B. Lee, Chin. J. Fluid Meas. **12**, 8 (1998); C. B. Lee, Phys. Lett. A **247**, 397 (1998); C. B. Lee, Chin. J. Atmos. Sci. **23**, 227 (1999); **23**, 55 (1999).
[20] C. B. Lee, Exp. Fluids **28**, 243 (2000); C. B. Lee, Chin. Phys. **9**, 508 (2000); C. B. Lee, Acad. Periodical Abstracts China **5**, 207 (1999); C. B. Lee, Chin. Phys. Lett. **17**, 583 (2000).
[21] C. B. Lee, Exp. Fluids (to be published).
[22] C. B. Lee, V. I. Borodulin, V. V. Gaponenko, and Y. S. Kachanov, in *Proceedings of the International Conference on Methods of Aerophysical Research* (Institute of Theoretical and Applied Mechanics, Novosibirsk, 1998); V. I. Borodulin, Y. S. Kachanov, C. B. Lee, and Q. X. Lian, J. Fluid Mech. (to be published).
[23] P. Moin, A. Leonard, and J. Kim, Phys. Fluids **29**, 954 (1986).
[24] C. R. Knapp and P. J. Roache, AIAA J. **6**, 29 (1968).
[25] R. E. Falco, Phys. Fluids **20**, s124 (1977).
[26] S. J. Kline, W. C. Reynolds, F. A. Schraub, and W. P. Runstadler, J. Fluid Mech. **30**, 741 (1967).
[27] Q. X. Lian, J. Fluid Mech. **215**, 101 (1990).
[28] E. R. Linden, Ark. Fys. **15**, 97 (1959).
[29] E. R. Linden, Ark. Fys. **15**, 503 (1959).
[30] M. V. Morkovin and E. Reshotko, in *Proceedings of the International Union of Theoretical and Applied Mechanics on Laminar-Turbulent Transition* (Ref. [6]).
[31] J. M. Kendall, AIAA Pap. 85-1695 (1985).
[32] M. Van Dyke, *An Album of Fluid Motion: Assembled of Mechanical Engineering* (The Parabolic Press, Stanford, 1988).
[33] Y. S. Kachanov and V. Y. Levchenko, J. Fluid Mech. **138**, 209 (1984).
[34] A. D. D. Craik, J. Fluid Mech. **50**, 393 (1971).
[35] M. B. Zelman and I. I. Maslennikova, J. Fluid Mech. **252**, 499 (1993).
[36] A. H. Nayfeh and A. N. Bozatli, Phys. Fluids **22**, 805 (1979).
[37] R. D. Joslin, C. R. Street, and C. L. Chang, Theor. Comput. Fluid Dyn. **4**, 171 (1993).
[38] C. H. K. Williamson, J. Fluid Mech. **243**, 393 (1992).
[39] C. H. K. Williamson and A. Prasad, Phys. Fluids A **5**, 1854 (1993).
[40] X. Wu and P. A. Stewart, J. Fluid Mech. **316**, 335 (1996).
[41] R. F. Blackwelder, Phys. Fluids **26**, 2807 (1983).
[42] Y. Fukunishi, H. Sato, and O. Inous, AIAA paper no. 87-1253 (1987).
[43] A. S. W. Thomas and W. S. Saric, Bull. Am. Phys. Soc. **26**, 1252 (1981).
[44] H. T. Kim, S. J. Kline, and W. C. Reynolds, J. Fluid Mech. **50**, 133 (1971).
[45] R. F. Blackwelder and J. H. Haritonidis, J. Fluid Mech. **132**, 87 (1983).
[46] S. C. Reddy, P. J. Schmid, J. S. Baggett, and D. S. Henningson, J. Fluid Mech. **365**, 269 (1998).
[47] R. E. Falco, Philos. Trans. R. Soc. London, Ser. A **336**, 103 (1990).
[48] C. R. Smith and S. P. Metzler, J. Fluid Mech. **129**, 27 (1983).
[49] J. H. Watmuff, J. Fluid Mech. **397**, 119 (1999).